



BYSL Promotes Glioblastoma Cell Migration, Invasion, and Mesenchymal Transition Through the GSK-3 β / β -Catenin Signaling Pathway

Zhuang Sha^{1,2†}, Junbo Zhou^{1,2†}, Yihao Wu^{1,2†}, Tong Zhang², Cheng Li^{1,2}, Qingming Meng², Preethi Priyanka Musunuru^{1,2}, Fangting You^{1,2}, Yue Wu^{1,2}, Rutong Yu^{1,2*} and Shangfeng Gao^{1,2*}

¹ Institute of Nervous System Diseases, The Affiliated Hospital of Xuzhou Medical University, Xuzhou Medical University, Xuzhou, China, ² Department of Neurosurgery, The Affiliated Hospital of Xuzhou Medical University, Xuzhou, China

OPEN ACCESS

Edited by:

Massimo Nabissi,
University of Camerino, Italy

Reviewed by:

Dusten Unruh,
Northwestern Medicine, United States
Claudia Katharina Petritsch,
Stanford University, United States

*Correspondence:

Rutong Yu
yu.rutong@163.com
Shangfeng Gao
gaoshangfeng@xzhmu.edu.cn

†These authors have contributed
equally to this work

Specialty section:

This article was submitted to
Neuro-Oncology and Neurosurgical
Oncology,
a section of the journal
Frontiers in Oncology

Received: 24 May 2020

Accepted: 31 August 2020

Published: 15 October 2020

Citation:

Sha Z, Zhou J, Wu Y, Zhang T, Li C,
Meng Q, Musunuru PP, You F, Wu Y,
Yu R and Gao S (2020) BYSL
Promotes Glioblastoma Cell Migration,
Invasion, and Mesenchymal Transition
Through the GSK-3 β / β -Catenin
Signaling Pathway.
Front. Oncol. 10:565225.
doi: 10.3389/fonc.2020.565225

BYSL, which encodes the human bystin protein, is a sensitive marker for astrocyte proliferation during brain damage and inflammation. Previous studies have revealed that BYSL has important roles in embryo implantation and prostate cancer infiltration. However, the role and mechanism of BYSL in glioblastoma (GBM) cell migration and invasion remain unknown. We found that knockdown of BYSL inhibited cell migration and invasion, downregulated the expression of mesenchymal markers (e.g., β -catenin and N-cadherin), and upregulated the expression of epithelial marker E-cadherin in GBM cell lines. Overexpression of BYSL promoted GBM cell migration, invasion, and epithelial-mesenchymal transition (EMT). In addition, the role of BYSL in promoting EMT was further confirmed in a glioma stem cell line derived from a GBM patient. Mechanistically, overexpression of BYSL increased the phosphorylation of GSK-3 β and the nuclear distribution of β -catenin. Inhibition of GSK-3 β by 1-Azakenpaullone could partially reverse the effects of BYSL downregulation on the transcriptional activity of β -catenin, the expression of EMT markers, and GBM cell migration/invasion. Moreover, immunohistochemical analysis showed strong expression of BYSL in GBM tissues, which was positively correlated with markers of mesenchymal GBM. These results suggest that BYSL promotes GBM cell migration, invasion, and EMT through the GSK-3 β / β -catenin signaling pathway.

Keywords: bystin, glioma, migration, invasion, GSK-3 β , EMT

INTRODUCTION

Glioma is the most common tumor of the central nervous system. Despite comprehensive treatments (surgical resection and chemoradiotherapy) to improve patient prognosis, the overall survival of patients with glioblastoma (GBM) remains poor (1–4), and aggressive growth and unregulated proliferation contribute to poor efficacy of treatment. Therefore, investigation of novel therapeutic targets to combat tumor growth and expansion is critical to improve the treatment of this currently incurable type of cancer.

BYSL, which encodes the bystin protein, is a highly conserved gene that has evolved from yeast to humans (5, 6). In humans, BYSL, together with adhesion molecules trophinin and tastin,

forms a complex that is highly expressed in trophoblast cells and endometrial cells of the utero-placental interface in early pregnancy and disappears in the second trimester of pregnancy (7). When embryos are transplanted, trophoblast cells actively proliferate and invade the uterine wall, promoting placenta formation and embryo implantation (8). This process is very similar to that of tumor invasion of surrounding tissues. It has been reported that BYSL has an oncogenic role in breast, prostate, liver, and ovarian cancer (9–12). Importantly, BYSL is highly expressed in neural infiltration models of prostate cancer (12).

Epithelial-mesenchymal transition (EMT) is a reversible biological process characterized by loss of polarized organization and acquisition of migratory and invasive capabilities (13, 14). Verhaak et al. classified GBM into four subtypes, proneural, neural, classical, and mesenchymal. The mesenchymal subtype is characterized by strong expression of mesenchymal markers (CHI3L1 and CD44) (15). These markers are reminiscent of an EMT that has been linked to dedifferentiated and transdifferentiated tumors (16).

WNT and β -catenin are highly expressed in GBM tissues and are associated with poor prognosis in patients with GBM (4, 17). The activation of WNT/ β -catenin leads to inhibition of the axin complex (axin/APC/CK1/GSK-3 β) and thus to the stabilization of β -catenin. The accumulated β -catenin translocates to the nucleus and activates the transcription of target genes, including Twist1/2, MMP7, and Survivin (18). WNT/ β -catenin signaling is involved in glioma cell invasion and EMT (19, 20).

In this study, we hypothesized that BYSL might contribute to GBM cell migration, invasion, and EMT *via* GSK-3 β / β -catenin signaling. We first investigated the role of BYSL in cell migration, invasion, and EMT in GBM cell lines using small interfering RNA (siRNA) and a lentivirus overexpressing BYSL. Then, we confirmed the promotion of EMT by BYSL in glioma stem cells (GSCs). Finally, we used 1-Azakenpauellone (a GSK-3 β inhibitor) to demonstrate the necessity of GSK-3 β activity in the regulation by BYSL of GBM cell migration, invasion, and EMT. In addition, clinical samples were used to detect the expression of BYSL in non-tumor brain tissues and GBM tissues, and to explore the correlation between BYSL and mesenchymal makers (e.g., CHI3L1 and CD44).

MATERIALS AND METHODS

Patients and Samples

All the GBM tissue specimens (obtained during surgical resection) and non-tumor brain tissue specimens (obtained from patients undergoing surgery for internal decompression after cerebral trauma) were collected from the Affiliated Hospital of Xuzhou Medical University. All the patients were naïve to immunotherapy, radiation, and chemotherapy. The specimens were fixed in 10% buffered formalin and embedded in paraffin for sectioning. Clinicopathological information for all participants is presented in **Supplementary Table 1**. All the GBM specimens were from patients with a confirmed pathological diagnosis, classified according to the criteria of the World Health Organization.

Cell Lines and Cell Culture

HEK 293T cells and human GBM cell lines U251 and U87 were purchased from the Shanghai Cell Bank, Type Culture Collection Committee, Chinese Academy of Sciences. The identities of the U251 and U87 cell lines were confirmed by DNA profiling test (STR). Cells were grown in Dulbecco's modified Eagle's medium (HEK 293T and U251) or minimal essential medium (U87) supplemented with 10% fetal bovine serum (Thermo Fisher Scientific, Waltham, MA). All cell lines were cultured in a cell incubator with a 5% CO₂ atmosphere under saturated humidity at 37 °C.

Reagents, Antibodies, and Plasmids

1-Azakenpauellone (1-Az, Selleck, Shanghai, S7193), Lipofectamine 2000 (Invitrogen, Carlsbad, CA), and PolyJet (SignaGen, Gaithersburg, MD) were purchased from the corresponding companies. The primary antibodies used for western blot were as follows: BYSL (1:500, Sigma, St. Louis, MO, HPA031217), β -catenin (1:2000, Cell Signaling Technology, Denver, CO, 8480s), N-cadherin (1:1000, Abcam, Cambridge, UK, ab98952), E-cadherin (1:1000, Proteintech, Rosemont, IL, 20874-1-AP), Slug (1:1000, Abcam, ab180714), Vimentin (1:1000, Santa Cruz Bio, Santa Cruz, CA, sc-373717), GSK-3 β (1:2000, Cell Signaling Technology, 9832S), p-GSK-3 β (1:2000, Cell Signaling Technology, 9323T), Flag (1:1000, Sigma, F1804), β -actin (1:1000, Santa Cruz Bio, sc-47778), GAPDH (1:20000, Proteintech, 60004-1-Ig), Histone H3 (1:1000, Cell Signaling Technology, 4499S). The Flag-tagged BYSL-overexpressing plasmid was purchased from Viogene Biosciences (Jinan, Shandong, China). TOP-Flash, FOP-Flash, and pGMLR-TK plasmids were obtained from GenScript (Hong Kong, China).

Transfection

For siRNA transfection, a previously validated BYSL siRNA (10) was synthesized by Biomics Biotech (Nantong, China). Cells were seeded in six-well plates at 50–70% confluence, and BYSL siRNA (siBYSL, 100 nM) or negative control (siNC, 100 nM) was transfected using Lipofectamine 2000 according to the protocol provided by the manufacturer.

For plasmid transfection, when the cells had grown to 70–90% confluence on a 6-cm plate, the plasmid (1 μ g) was transfected using PolyJet (3 μ L) according to the manufacturer's instructions.

Lentivirus Construction, Production, and Infection

Human BYSL (accession number: NM_004053) was inserted into the pCDH-GFP-puro vector plasmid at the Nhe I and Bgl II sites. The lentiviruses were produced in HEK293T cells and used to infect GBM cells according to our previously reported protocol (21). Forty-eight hours (h) after infection, the infected cells were cultured in medium containing 2.5 μ g/mL puromycin (Sigma) for selection. The surviving cells were used in the subsequent experiments.

Wound Healing Assay

Cells were seeded in a six-well plate and incubated at 37 °C until they reached 80–90% confluence. A wounding line was scratched

with a 200 μ L pipette tip, and the dead cells were washed with phosphate-buffered saline (PBS). Then, serum-free DMEM was added to each well. The migrating cells were monitored using an IX-71 inverted microscope (Olympus, Tokyo, Japan). Images were taken in three randomly selected fields at 0, 24, and 48 h. The number of migrating cells was counted based on the captured images using ImageJ software (National Institutes of Health, Bethesda, MD).

Transwell Assay

To assess cell migration and invasion, a transwell assay was performed in a 24-well chamber system with a polycarbonate membrane (Corning, Corning, NY) as described in the literature (22, 23). Briefly, 200 μ L of serum-free medium was added to the upper chamber containing 1×10^4 cells. The lower chamber was filled with 500 μ L of medium containing 10% fetal bovine serum and then incubated at 37 °C for 24 or 48 h. To assess invasion ability, Matrigel (BD, Franklin Lakes, NJ) was pre-coated onto the polycarbonate membrane; the rest of the procedure remained the same. The migrating and invading cells were counted on the captured images as described previously (21).

RNA Extraction and Quantitative Real-Time PCR (qRT-PCR)

Total RNA was extracted from cultured cells using TRIzol (Invitrogen) according to the instructions provided by the manufacturer. We employed a Prime Script RT Reagent Kit (TAKARA, Dalian, China) to perform the reverse transcription. The target gene was amplified in a final volume of 20 μ L with a SYBR Green PCR Master mix (TAKARA). The qRT-PCR reaction was run in an Applied Biosystems 7500 Real-Time PCR System (Waltham, MA), and data were collected automatically. Forward and reverse primers for all genes are given in **Supplementary Table 2**. The expression of target genes was normalized to that of β -actin, and relative absolute amounts of target genes were calculated according to our previous method for statistical analysis (24).

Protein Extraction and Western Blot

Cells were washed in PBS and lysed in ice-cold lysis buffer to obtain whole-cell protein. Cytoplasmic and nuclear proteins were extracted using a commercial kit (Beyotime Biotech Inc, Nantong, China) according to the manufacturer's instructions. Equal amounts of total protein were loaded for western blot analysis according to a protocol similar to that described in our recently published paper (21). The source and dilution ratio of the primary antibodies were as described in the section "Reagents, antibodies, and plasmids." Band densities were quantified using the ImageJ software. β -actin or GAPDH was used as a loading control for cytoplasmic protein, and Histone H3 was used as a loading control for nuclear protein.

GSCs Culture and Neurosphere Formation Assay

Glioma tissue samples were obtained from an IDH1-wildtype GBM patient (male, 53 years old) during surgery. His GSCs (named GSC-F) were established and cultured as previously

described (25). In brief, GBM tissues were washed, minced, and enzymatically dissociated, after which the tumor cells were suspended in stem cell medium (SCM) (DMEM/F12 medium with 2% B27 (Thermo Fisher Scientific), 1% N2 (Thermo Fisher Scientific), 20 ng/mL EGF and bFGF (Peprotech, Rocky Hill, NJ), HEPES (final concentration of 5 mM), and 1% penicillin/streptomycin solution. The neurosphere formation assay was performed as follows. GSC-F cells were dissociated into single cells at a concentration of 10,000–50,000 cells/mL, and 200 μ L of the cell suspension was added to each well of a 96-well plate. The SCM was replaced every 3–4 days. After 6–8 days, neurospheres (diameter $\geq 50 \mu$ m) in each well were counted.

TOP/FOP-Flash Reporter Assay

We used a TOP/FOP-Flash reporter assay to detect the transcriptional activity of β -catenin as described previously (19). Briefly, cells were seeded in a 96-well plate and transfected with siBYSL or siNC in the presence of reporter plasmids containing TOP-Flash or mutated FOP-Flash TCF/LEF DNA-binding sites and pGMLR-TK plasmid. The groups were as follows: siNC + TOP-Flash + pGMLR-TK + DMSO group, siNC + FOP-Flash + pGMLR-TK + DMSO group, siBYSL + TOP-Flash + pGMLR-TK + DMSO group, siBYSL + FOP-Flash + pGMLR-TK + DMSO group, siNC + TOP-Flash + pGMLR-TK + 1-Az group, siNC + FOP-Flash + pGMLR-TK + 1-Az group, siBYSL + TOP-Flash + pGMLR-TK + 1-Az group, siBYSL + FOP-Flash + pGMLR-TK + 1-Az group. A dual luciferase reporter assay system (Promega, Madison, WI) was used to measure luciferase activity 24 h after transfection. The luciferase activity of each sample was normalized to the respective Renilla luciferase activity.

5-Ethynyl-20-Deoxyuridine (EdU) Incorporation Assay

The EdU assay was performed using a commercial kit (RiboBio, Guangzhou, China), as described in the literature (26). The percentage of EdU-positive cells was calculated by dividing the number of EdU-positive cells by the number of Hoechst-stained cells.

Immunohistochemistry and Cell Counting

The immunoreactivity (IR) of BYSL, CD44, and CHI3L1 was detected by immunohistochemistry and quantified by cell counting, as described in our previous publications (21, 27). Briefly, antigen retrieval was applied to sections in citrate buffer (pH 6.0) with microwaves. Primary antibodies against BYSL (1:50, Sigma), CD44 (1:100, OriGene, Rockville, MD), and CHI3L1 (1:50, Proteintech) were added. All sections were then processed using an ABC Elite kit (Vector Laboratories, Burlingame, CA) according to the manufacturer's protocol. Finally, the sections were counterstained with hematoxylin (KeyGEN BioTECH, Jiangsu, China). All images were captured using a DM2500 microscope (Leica, Wetzlar, Germany), and cell counting was performed by an investigator without knowledge of the identity of any of the subjects.

Statistical Analysis

In vitro experiments were repeated at least three times, and data are expressed as mean \pm S.D. Comparisons between two groups were performed by Student's *t*-test. Differences among multiple groups were determined by one-way analysis of variance followed by Dunnett's or Tukey *post hoc* test. Correlations were analyzed by Spearman correlation test. Statistical analyses were performed using SPSS version 19.0 (SPSS Inc., Chicago, IL). Tests were two-tailed, and values of $P < 0.05$ were considered to be statistically significant.

RESULTS

Downregulation of BYSL Inhibits GBM Cell Migration and Invasion

We used a previously validated siRNA for targeting BYSL (10). Western blot and qRT-PCR analyses showed that BYSL was successfully downregulated by the siRNA in both U251 and U87 cells (Supplementary Figure 1). Wound healing and transwell assays were used to assess the effects of downregulation of BYSL on GBM cell migration and invasion. The results of the wound healing assay showed that knockdown of BYSL led to a significant $\sim 40\%$ decrease in the number of migrating cells at 24 and 48 h (all $P < 0.001$) in U251 cells (Figures 1A,B). The transwell assay showed that the numbers of cells migrating to the chamber and crossing the Matrigel were significantly decreased in U251 (percent-change $\sim 50\%$, all $P < 0.001$) and U87 (percent-change $> 60\%$, all $P < 0.001$) cells after BYSL was downregulated (Figures 1C–F). These results suggest that downregulation of BYSL inhibits GBM cell migration and invasion.

Downregulation of BYSL Inhibits the EMT in GBM Cells

As EMT is closely involved in the aggressive growth of GBM (19, 20), we next detected the expression of mesenchymal and epithelial markers in GBM cells. When BYSL was effectively downregulated by the siRNA, the mRNA levels of mesenchymal markers were significantly reduced in U251 cells (β -catenin: $P = 0.006$, N-cadherin: $P = 0.003$, Slug: $P = 0.003$, Vimentin: $P = 0.011$) and U87 cells (β -catenin: $P = 0.038$, N-cadherin: $P = 0.029$, Slug: $P < 0.001$, Vimentin: $P < 0.001$), whereas E-cadherin, an epithelial marker, was significantly upregulated in U251 cells ($P = 0.022$) and U87 cells ($P = 0.049$; Figures 2A,B). Furthermore, we found that knockdown of BYSL caused a significant 20% decrease in the protein levels of β -catenin ($P = 0.028$) and N-cadherin ($P = 0.039$) in U251 cells, a significant 12% decrease in the β -catenin ($P = 0.017$) and N-cadherin ($P = 0.024$) protein levels in U87 cells, and a significant 50% increase in the E-cadherin protein levels (U251: $P = 0.046$, U87: $P = 0.003$), with no significant effects on other mesenchymal markers (Figures 2C–F). These data suggest that downregulation of BYSL suppresses the EMT in GBM cells.

Overexpression of BYSL Promotes GBM Cell Migration and Invasion

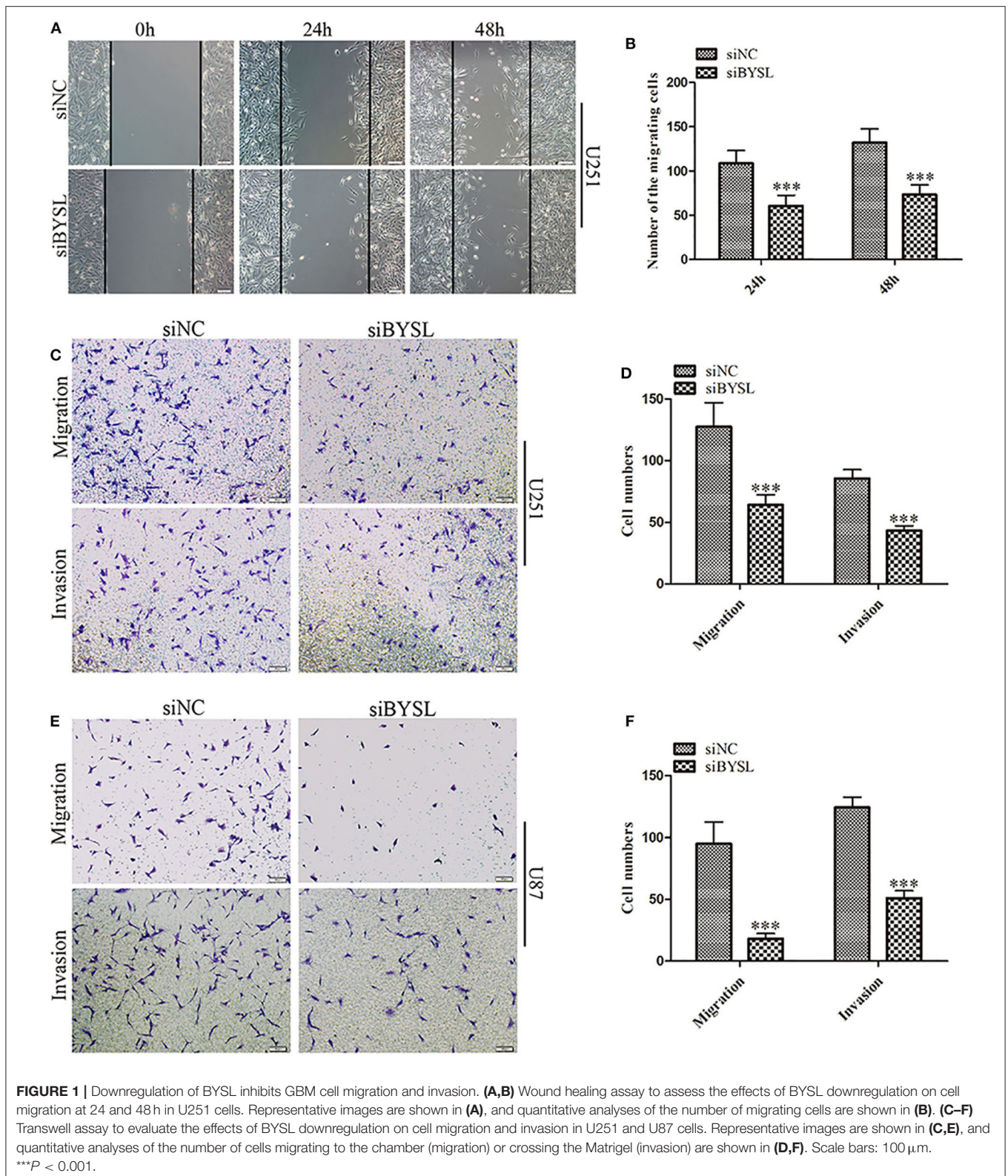
We established stable GBM cell lines with overexpression of BYSL by lentivirus-mediated infection in U251 and U87 cells. The number of cells with GFP fluorescence accounted for $\sim 90\%$ of total cells, as observed by fluorescence microscopy. Western blot analysis showed that exogenous BYSL was abundantly overexpressed in U251 and U87 cells (Supplementary Figure 2). Then, wound healing and transwell assays were used to evaluate the influence of BYSL overexpression on the migration and invasion of GBM cells. The wound healing assay showed that the numbers of migrating cells of U251 cells in the BYSL-overexpressing group were increased at 24 h (percent-change $\sim 100\%$) and 48 h (percent-change $\sim 40\%$) compared with the vector group (all $P < 0.001$, Figures 3A,B). The transwell assay showed that overexpression of BYSL led to a significant increase in the number of cells migrating to the chamber (percent-change $> 85\%$), and a significant increase in the number of cells crossing the Matrigel (percent-change $> 45\%$) in U251 and U87 cells (all $P < 0.001$, Figures 3C–F). These results indicate that overexpression of BYSL enhances the migration and invasion abilities of GBM cells.

Overexpression of BYSL Promotes the EMT in GBM Cells

We next used qRT-PCR and western blot analyses to measure the effects of BYSL overexpression on the expression of the EMT markers in GBM cells. The qRT-PCR assay showed that mRNA levels of mesenchymal markers were significantly increased in U251 cells (β -catenin: $P = 0.004$, N-cadherin: $P = 0.002$, Slug: $P < 0.001$, Vimentin: $P < 0.001$) and U87 cells (β -catenin: $P = 0.033$, N-cadherin: $P = 0.019$, Slug: $P = 0.006$, Vimentin: $P < 0.001$), whereas E-cadherin mRNA expression was significantly downregulated (U251: $P = 0.040$; U87: $P = 0.024$) in the BYSL-overexpressing group (Figures 4A,B). Furthermore, overexpression of BYSL significantly increased the protein levels of β -catenin (percent-change $\sim 30\%$; U251: $P = 0.045$, U87: $P = 0.019$) and N-cadherin (percent-change $\sim 40\%$; U251: $P = 0.043$, U87: $P = 0.003$), decreased E-cadherin protein levels (percent-change $\sim 20\%$; U251: $P = 0.030$, U87: $P = 0.096$), and showed no significant effects on other mesenchymal markers (Figures 4C–F). These data suggest that the overexpression of BYSL triggers the expression of EMT activators in GBM cells.

Downregulation (Overexpression) of BYSL Inhibits (Promotes) Neurosphere Formation and the EMT in GSCs

To confirm the role of BYSL in promoting EMT, we performed a neurosphere formation assay and measured the expression of EMT markers in a patient-derived GSC cell line (GSC-F). Immunofluorescence staining showed positive expression of Nestin and CD44 in the GSC-F cells (Supplementary Figure 3). Downregulation of BYSL significantly decreased the number (percent-change $\sim 30\%$, $P < 0.001$) and size (percent-change $\sim 23\%$, $P = 0.002$) of neurospheres in the GSCs, whereas overexpression of BYSL showed the opposite effects



(Figures 5A–D). Furthermore, the qRT-PCR assay showed that knockdown of BYSL caused significant decreases in mRNA levels of β -catenin ($P = 0.043$), N-cadherin ($P = 0.007$), Slug ($P =$

0.041), and Vimentin ($P = 0.049$), and a significant increase in the E-cadherin mRNA level ($P < 0.001$) in GSC-F cells **(Figure 5G)**. Consistently, there were also significant changes in

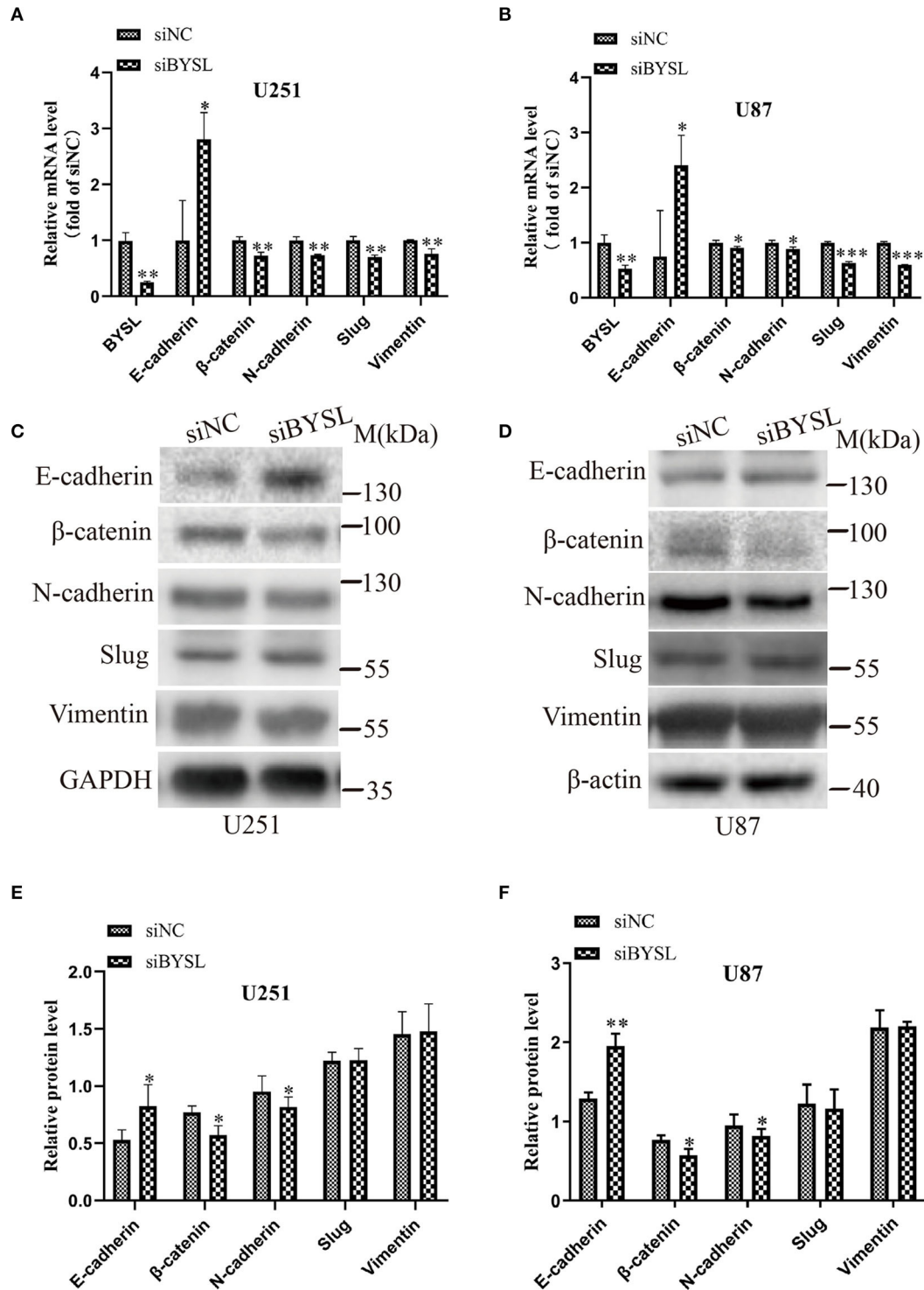


FIGURE 2 | Downregulation of BYSL inhibits the EMT in GBM cells. **(A,B)** QRT-PCR assay to measure changes in the mRNA levels of EMT markers (E-cadherin, β-catenin, N-cadherin, Slug, and Vimentin) in U251 and U87 cells following BYSL downregulation. **(C–F)** Western blot analyses to determine changes in the protein levels of EMT markers in U251 and U87 cells after silencing of BYSL. Representative blot images are shown in **(C,D)**. Quantification graphs are shown in **(E,F)**. M, molecular marker. **P* < 0.05, ***P* < 0.01, ****P* < 0.001.

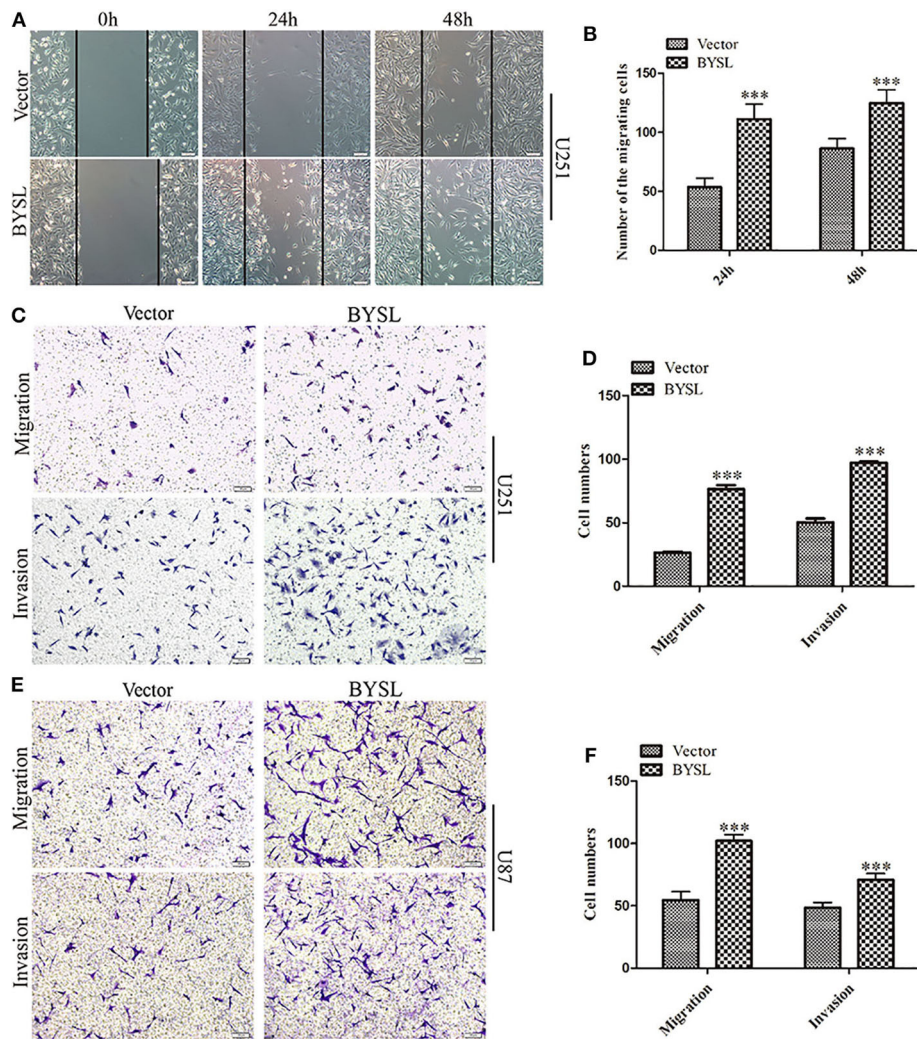


FIGURE 3 | Overexpression of BYSL promotes GBM cell migration and invasion. **(A,B)** Wound healing assay to assess the effects of BYSL overexpression on cell migration at 24 and 48 h in U251 cells. Representative images are shown in **(A)**, and quantitative analyses of the number of migrating cells are shown in **(B)**. **(C–F)** Transwell assay to evaluate the effects of BYSL overexpression on cell migration and invasion in U251 and U87 cells. Representative images are shown in **(C,E)** and quantitative analyses of the number of cells migrating to the chamber (migration) or crossing the Matrigel (invasion) are shown in **(D,F)**. Scale bars: 100 μm . *** $P < 0.001$.

the protein levels of β -catenin and N-cadherin (percent-change $> 30\%$, all $P = 0.004$), and E-cadherin (percent-change $\sim 50\%$, $P < 0.001$; **Figures 5E,H**). On the contrary, overexpression of BYSL caused a significant $\sim 50\%$ increase in the protein levels of β -catenin and N-cadherin (all $P < 0.001$) and a significant $\sim 50\%$ decrease in the E-cadherin protein levels ($P = 0.032$) in GSC-F cells (**Figures 5E, I**). These results further confirm the role of BYSL in promoting EMT of GBM cells.

Overexpression of BYSL increases the activity of GSK-3 β / β -catenin signaling pathway

As GSK-3 β is an important component of the axin degradation complex, which determines whether β -catenin is transported into the nucleus or undergoes proteasome-dependent degradation

(28–31), we next examined the levels of phosphorylated GSK-3 β (p-GSK-3 β) and total GSK-3 β in GBM cell lines. Overexpression of BYSL significantly elevated p-GSK-3 β levels in U251 cells (percent-change $\sim 30\%$, $P = 0.024$) and U87 cells (percent-change $\sim 130\%$, $P = 0.025$), without affecting the total GSK-3 β levels (**Figures 6A–D**). Moreover, upregulation of BYSL promoted the nuclear distribution of β -catenin in U87 cells ($P = 0.015$, **Figures 6E–H**). These results imply that GSK-3 β / β -catenin signaling is located downstream of BYSL in GBM cells.

Inhibiting GSK-3 β Could Partially Reverse the Diminished β -Catenin Activity Caused by BYSL Downregulation

Consistent with the nuclear translocation of β -catenin following BYSL overexpression, the TOP/FOP-Flash reporter assay

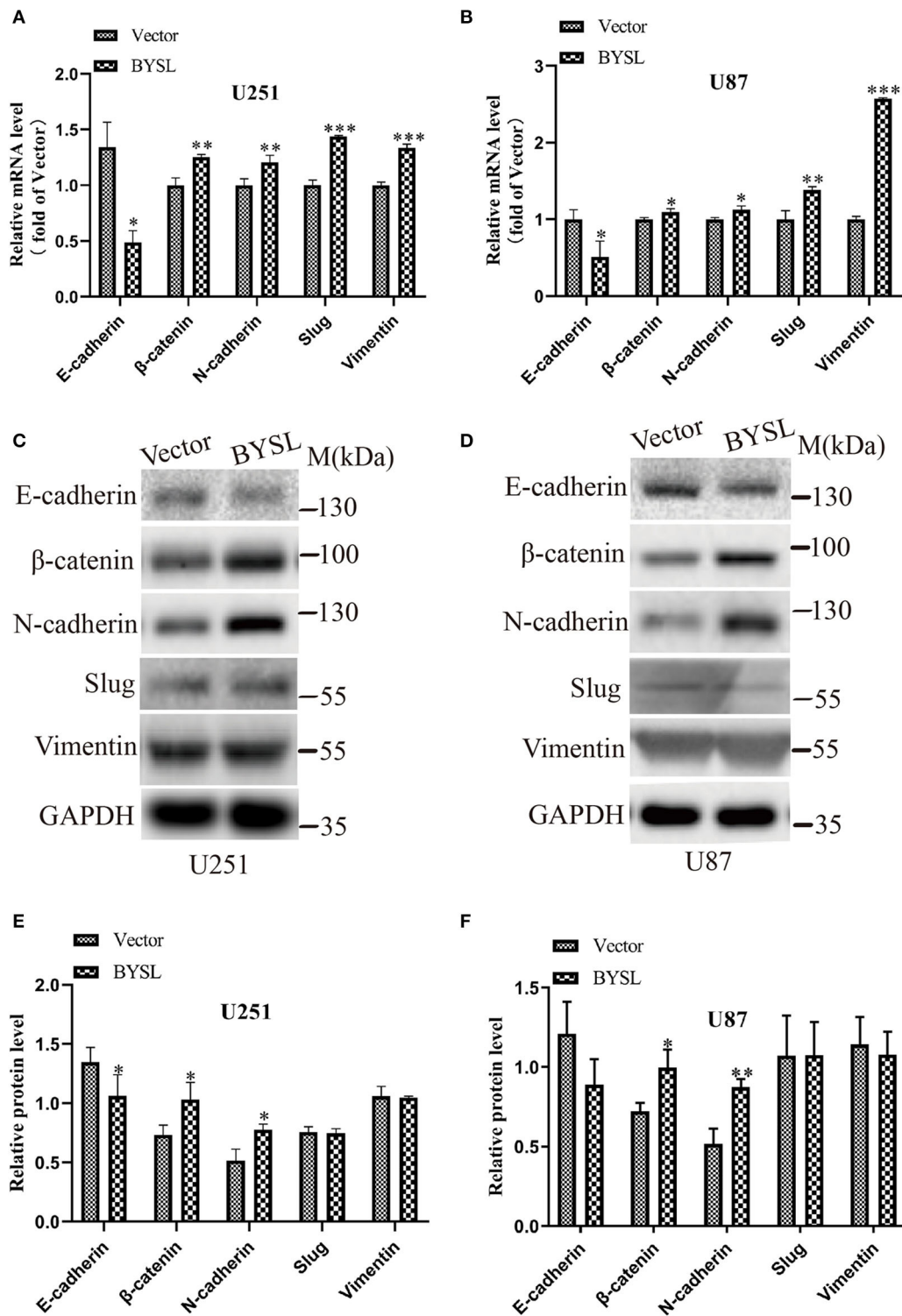


FIGURE 4 | Overexpression of BYSL promotes the EMT in GBM cells. **(A,B)** QRT-PCR assay to measure the mRNA levels of EMT markers (E-cadherin, β -catenin, N-cadherin, Slug, and Vimentin) in U251 and U87 cells following BYSL overexpression. **(C-F)** Western blot analyses to determine the protein expression of EMT markers in BYSL-overexpressing U251 and U87 cells. Representative blot images are shown in **(C,D)**. Quantification graphs are shown in **(E,F)**. M, molecular marker. * $P < 0.05$, ** $P < 0.01$, *** $P < 0.001$.

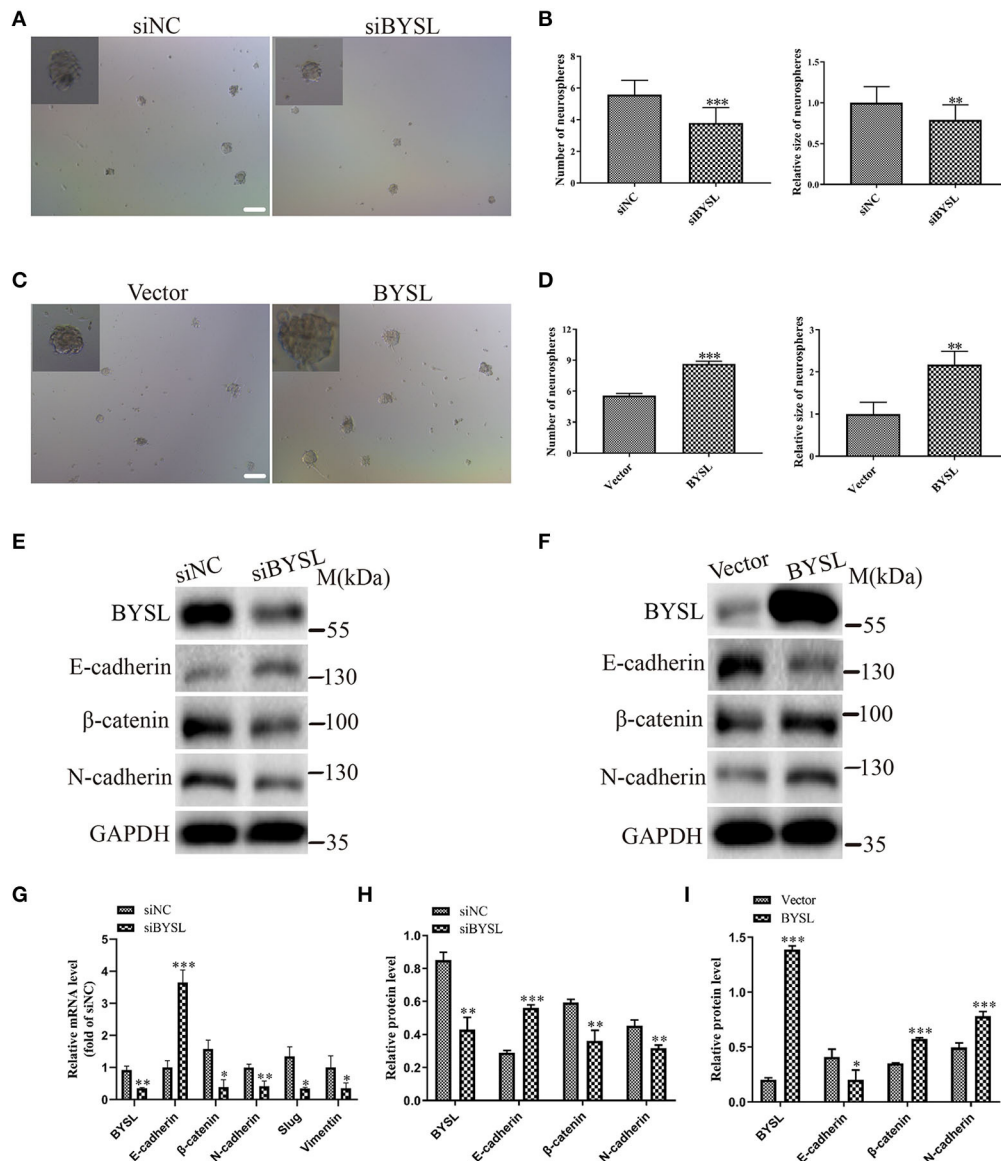


FIGURE 5 | Downregulation (overexpression) of BYSL inhibits (promotes) tumorsphere formation and the EMT process in GSCs. **(A–D)** Neurosphere formation assay in GSC-F cells to evaluate the role of BYSL in neurosphere formation. Representative images are shown in **(A,C)**, and quantitative analyses of the number and size of spheroids are shown in **(B,D)**. Scale bars: 100 μm. **(E–I)** Western blot and qRT-PCR assays to determine the expression changes of EMT markers in the BYSL-silencing/overexpressing GSC-F cells. Representative blot images are shown in **(E,F)**. Quantification graphs are shown in **(G–I)**. M, molecular marker. * $P < 0.05$, ** $P < 0.01$, *** $P < 0.001$.

showed that the transcriptional activity of β -catenin was significantly repressed in HEK293T cells following knockdown of BYSL (percent-change $\sim 12\%$, $P = 0.005$, **Figure 7A**). More importantly, treatment with 1 μM 1-Az (an inhibitor of GSK-3 β) reversed the decrease in β -catenin activity caused by downregulation of BYSL (percent-change $\sim 20\%$, $P = 0.020$, **Figure 7A**). Furthermore, the qRT-PCR assay showed that the transcription of the β -catenin target genes

was significantly reduced following BYSL downregulation (Twist-1: $P < 0.001$, Twist-2: $P = 0.011$, MMP7: $P = 0.009$, Survivin: $P < 0.001$); this reduction was partially reversed by 1-Az administration (Twist-1: $P < 0.001$, Twist-2: $P = 0.001$, MMP7: $P < 0.001$, Survivin: $P = 0.146$) in U87 cells (**Figure 7B**). These results indicate that GSK-3 β activity is required for BYSL-mediated β -catenin activation in GBM cells.

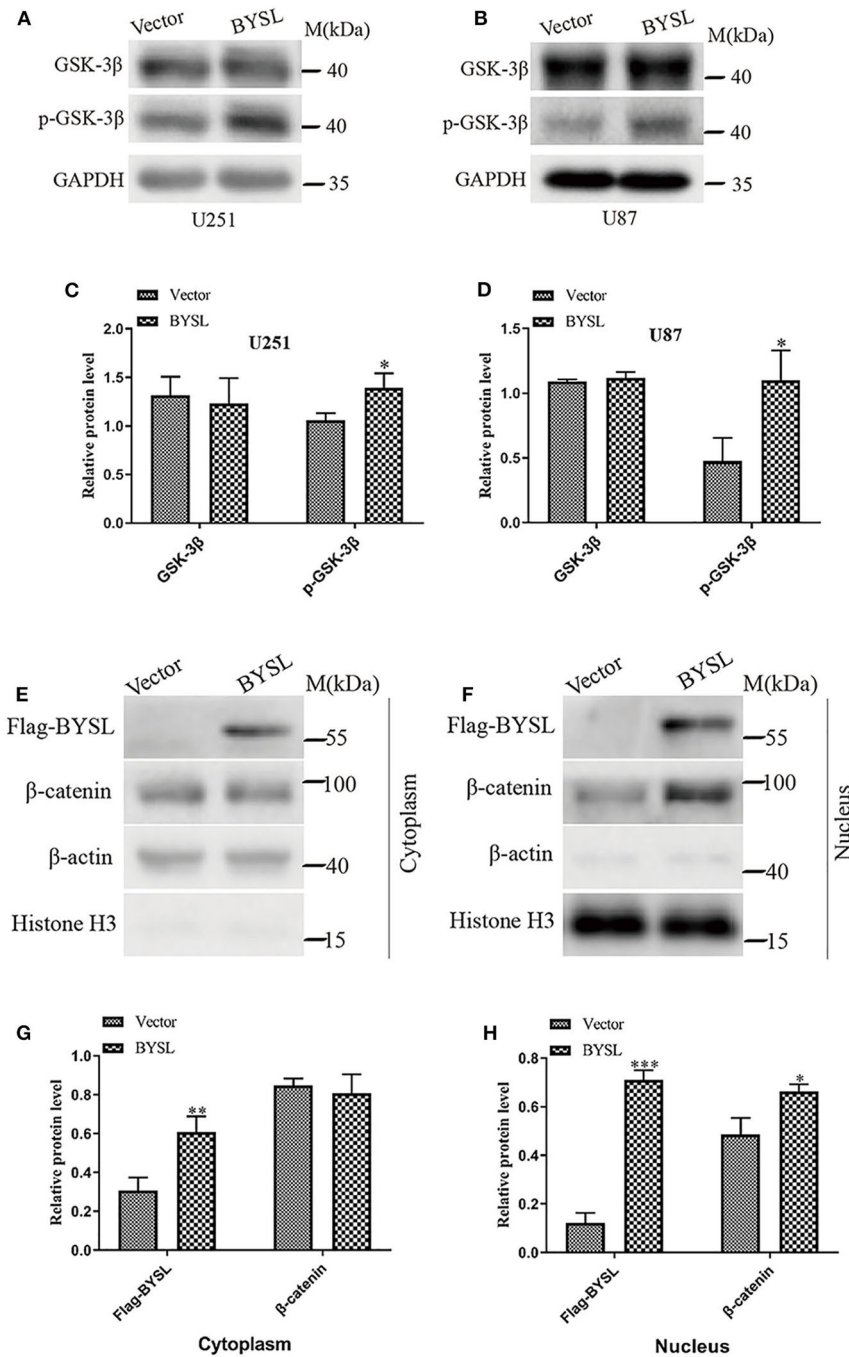
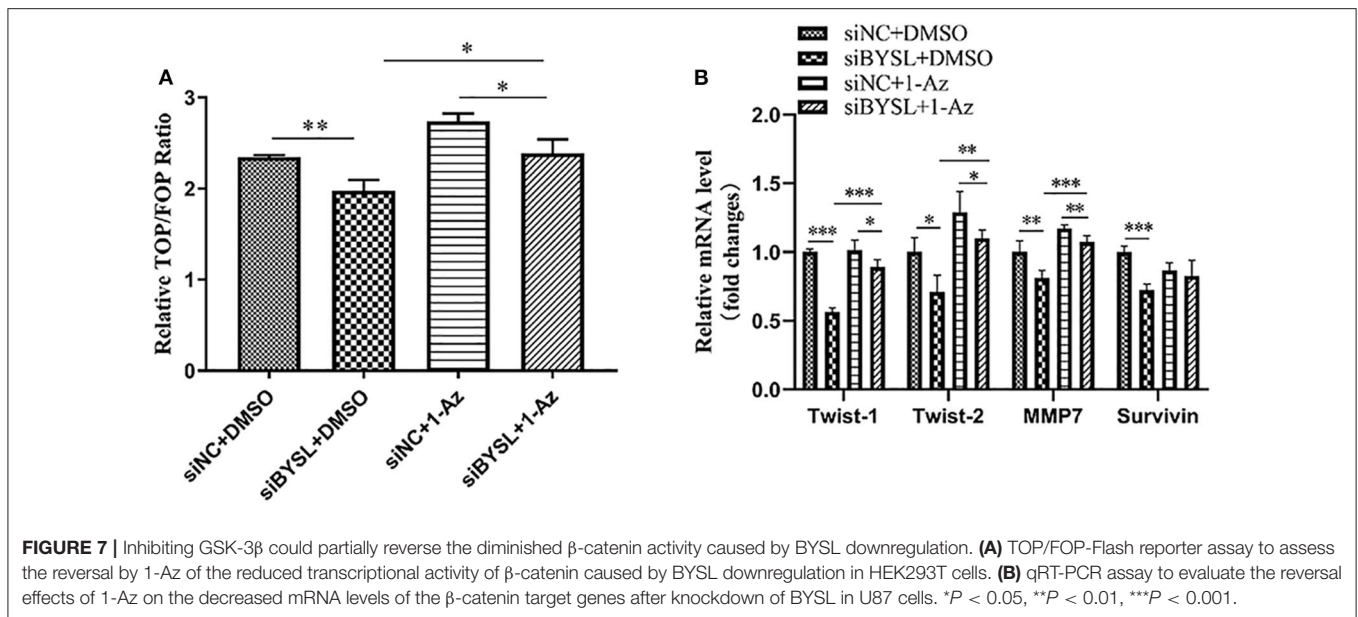


FIGURE 6 | Overexpression of BYSL enhances the activity of GSK-3β/β-catenin signaling pathway in GBM cells. **(A–D)** Western blot analyses to measure the levels of p-GSK-3β and GSK-3β in U251 and U87 cells. Representative blot images are shown in **(A,B)**. Quantification graphs are shown in **(C,D)**. **(E–H)** Distribution of β-catenin in cytoplasm and nucleus as detected by western blot analysis. Representative blot images are shown in **(E,F)**. Quantification graphs are shown in **(G,H)**. M, molecular marker. **P* < 0.05, ***P* < 0.01, ****P* < 0.001.

Inhibiting GSK-3β Could Partially Reverse the Effects of BYSL Downregulation on GBM Cell Migration, Invasion, and EMT

Western blot analysis showed that downregulation of BYSL resulted in a significant ~20% decrease in the protein levels of

mesenchymal markers (β-catenin: *P* = 0.026, N-cadherin: *P* = 0.005) in U87 cells (**Figures 8A,B**), consistent with the results shown in **Figures 2D–F**. Inhibition of GSK-3β by 1-Az partially reversed ~20% decrease in protein levels of mesenchymal markers caused by downregulation of BYSL (β-catenin: *P* =



0.037, N-cadherin: $P = 0.008$). We next used transwell assays to assess the reversal effects of 1-Az on the decrease in cell migration and invasion caused by BYSL downregulation in GBM cells. Consistent with our findings shown in **Figures 1E, F**, downregulation of BYSL resulted in a significant $\sim 45\%$ decrease in the number of migrating- and invading-U87 cells (all $P < 0.001$, **Figures 8C,E**). Treatment with 1-Az partially reversed the decrease in migration and invasion ability caused by BYSL downregulation (all $P < 0.001$, **Figures 8C,E**). In addition, the EdU assay revealed a significant inhibitory effect of BYSL downregulation on the percentage of EdU-positive cells in U87 cells (percent-change $\sim 46\%$, $P < 0.001$, **Figures 8D,F**); however, this effect could not be reversed by 1-Az (**Figures 8D,F**). These data suggest that BYSL promotes GBM cell migration, invasion, and EMT *via* the GSK-3 β / β -catenin signaling pathway.

Strong Expression of BYSL Is Associated With the Mesenchymal GBM Subtype

The IR of BYSL was analyzed by immunohistochemistry followed by cell counting in non-tumor brain tissues and GBM tissues ($n = 11$ for each group). BYSL-IR was located in both cytoplasm and nucleus, and the percentage of BYSL-IR cells was significantly increased in GBM tissues ($P < 0.001$, **Figures 9A,B**). In addition, immunohistochemical data for CD44 and CHI3L1 were available for the GBM tissues (**Figure 9A**). Nine of the 11 GBM tissue samples were of mesenchymal subtype, as indicated by strong expression of CD44 and CHI3L1. BYSL was positively correlated with CD44 ($\rho = 0.727$, $P = 0.027$) and CHI3L1 ($\rho = 0.655$, $P = 0.055$) in the mesenchymal GBM subtype (**Figures 9C,D**). These findings suggest that BYSL is highly expressed in GBM, especially in the mesenchymal subtype.

DISCUSSION

In this study, we demonstrated that overexpression of BYSL promoted GBM cell migration/invasion and enhanced EMT. Silencing of BYSL showed the opposite effects. The GSK-3 β / β -catenin signaling pathway was regulated by BYSL and was required for the promotion by BYSL of GBM cell migration/invasion and EMT. In addition, high expression of BYSL was found in GBM tissues and was positively correlated with mesenchymal markers CD44 and CHI3L1. Collectively, these results suggest that BYSL promotes GBM cell migration, invasion, and EMT through the GSK-3 β / β -catenin pathway.

BYSL is upregulated in reactive astrocytes in response to brain injury or inflammation (32) and promotes liver cancer cell survival and tumorigenesis (10). In addition, BYSL promotes the growth and invasion of prostate cancer cells (12). In agreement with these findings, the current study showed that BYSL promoted the migration and invasion of GBM cells. Thus, BYSL is generally involved in the malignant progression of cancers.

The acquisition of EMT causes cell morphology to switch from a non-polar epithelial phenotype to a mesenchymal phenotype that is conducive to migration. This transition plays an important part in the infiltration and metastasis of tumor cells (13, 33). A number of epithelial and mesenchymal biomarkers are used to assess EMT in GBM cells (13). Our study demonstrated that knockdown of BYSL suppressed the expression of mesenchymal markers β -catenin and N-cadherin, and enhanced the expression of epithelial marker E-cadherin in GBM cells. Overexpression of BYSL showed the opposite effects. In addition, the role of BYSL in promoting EMT was further confirmed in a patient-derived GSC cell line. These results suggest that BYSL promotes EMT in GBM cells.

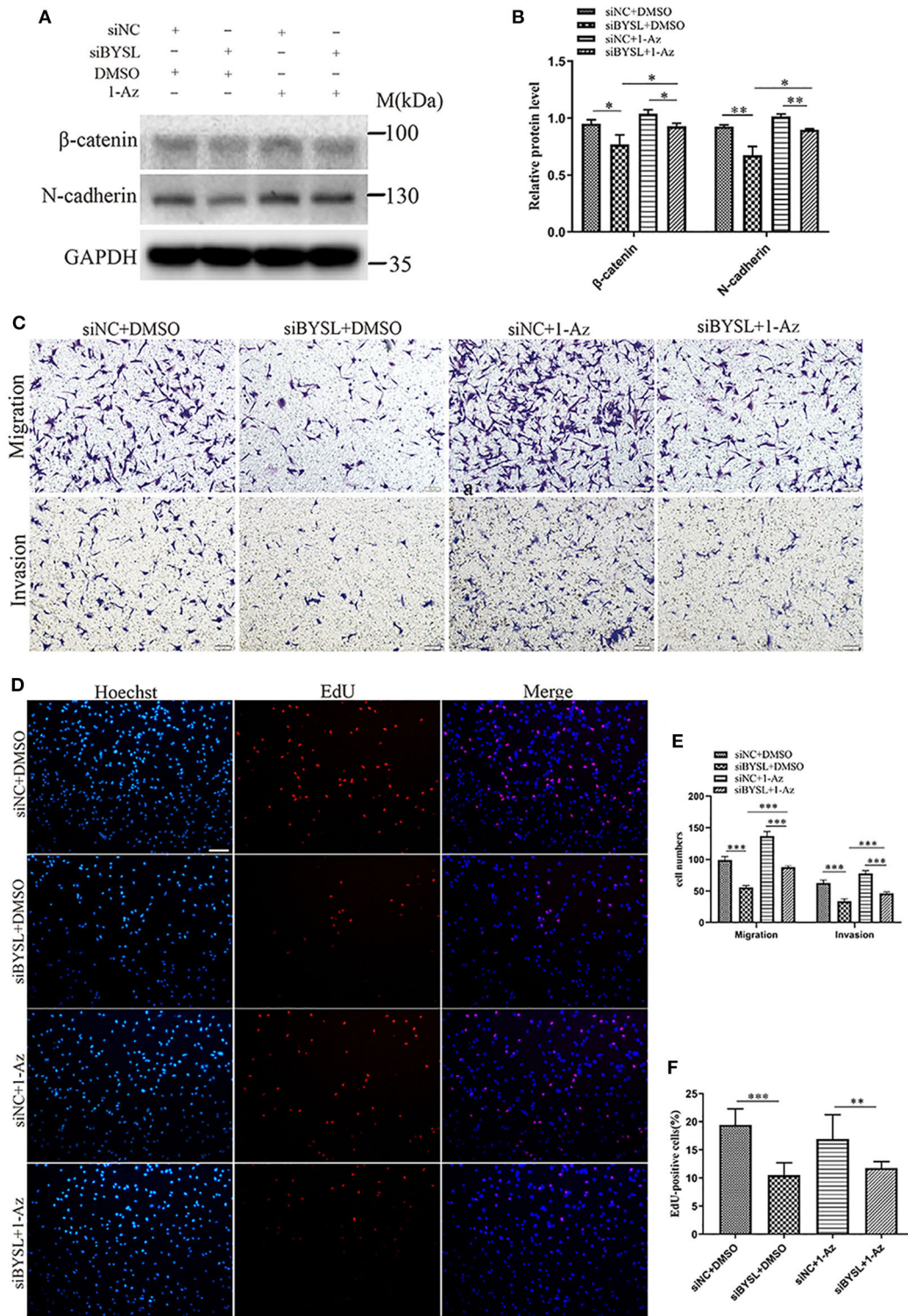


FIGURE 8 | Inhibiting GSK-3β could partially reverse the effects of BYSL downregulation on GBM cell migration, invasion, and EMT. **(A,B)** Western blot analyses to evaluate the reversal by 1-Az of the decrease in β-catenin and N-cadherin levels caused by BYSL downregulation in U87 cells. Representative blot images are shown in **(A)**. Quantification graph is shown in **(B)**. **(C,E)** Transwell assays to assess the reversal by 1-Az of the decreased cell migration and invasion caused by silencing of BYSL in U87 cells. Representative images are shown in **(C)**, and quantitative analyses of the number of cells migrating to the chamber (migration) or crossing the Matrigel (invasion) are shown **(E)**. **(D,F)** EdU assays to evaluate the effects of BYSL downregulation on cell proliferation and the reversal effects mediated by 1-Az treatments in U87 cells. Representative images are shown in **(D)**, and quantitative analyses of the percentages of EdU-positive cells are shown in **(F)**. Scale bars: 100 μm. M, molecular marker. **P* < 0.05, ***P* < 0.01, ****P* < 0.001.

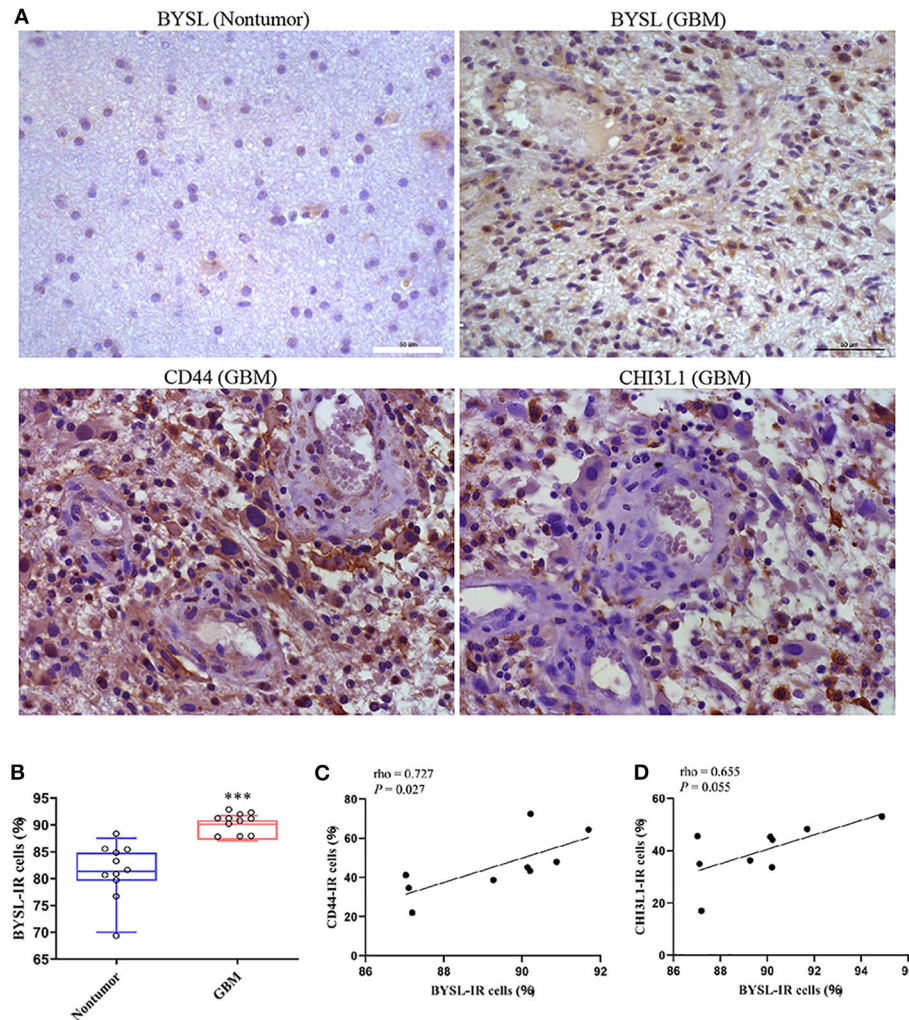


FIGURE 9 | BYSL is upregulated in GBM and associated with the GBM mesenchymal subtype. Immunohistochemical analysis to measure the IR of BYSL, CD44, and CHI3L1 in non-tumor brain tissues and/or GBM tissues. **(A)** Representative images for the BYSL-, CD44-, and CHI3L1-IR staining. **(B)** Cell counts showing that the percentage of BYSL-IR cells was significantly increased in GBM tissues compared with non-tumor brain tissues. **(C,D)** Spearman correlation analysis showing an association of BYSL with markers of mesenchymal GBM subtype (CD44 and CHI3L1). Scale bars: 50 μm . *** $P < 0.001$.

β -catenin is not only a hallmark of EMT but also an effector of the WNT/ β -catenin signaling pathway (28, 34, 35). It has been suggested that WNT signaling contributes to mesenchymal transition, migration, and invasion in glioma cells (17, 19). GSK-3 β is an important component of the axin degradation complex that determines β -catenin subcellular localization and activity (31, 35). Here, we found that overexpression of BYSL led to a significant increase in the phosphorylation of GSK-3 β and the nuclear distribution of β -catenin. In line with this, the activity of β -catenin and the transcription of its target genes were significantly decreased in GBM cells when BYSL was downregulated. A selective GSK-3 β inhibitor (36), 1-Az, could partially reverse these effects. These findings indicate that GSK-3 β activity is required for BYSL-mediated β -catenin signal transduction in GBM cells.

GSK-3 β is an AKT substrate, and AKT/GSK-3 β signaling is known to be involved in EMT (37, 38). We found that inhibiting GSK-3 β using 1-Az partially reversed the decrease in cell migration/invasion and EMT caused by BYSL downregulation, indicating that GSK-3 β activity is required for the promotion by BYSL of migration, invasion, and EMT in GBM cells. As AKT could affect EMT directly or through GSK-3 β (37), further investigations are needed to elucidate the role of BYSL in regulating AKT activity in GBM cells.

BYSL is highly expressed in liver cancer, in ovarian cancer tissues, and in prostate cancer cells near the peripheral nerves. Here, we found an upregulation of BYSL-IR in GBM. These results suggest that high expression of BYSL may be universally found in different cancer types. More importantly, BYSL showed

positive correlations with CD44 and CHI3L1 in GBM. Both of these molecules are markers of the mesenchymal subtype of GBM (15, 39), which is characterized by a higher percentage of necrotic cells and associated inflammation (15). Thus, these results provide further evidence for the association of BYSL with the highly invasive features of the mesenchymal GBM subtype.

In this study, we used a previously validated siRNA to knock down BYSL (10). Although downregulation of BYSL had significant effects on cell migration, invasion, and EMT, the differences were small or the variation was large for some data. This may have been caused by the limitations of RNA interference. We also attempted experiments in a stable cell line mediated by shRNA lentivirus, but the cells stably silencing BYSL grew slowly or died, so they could not be used for functional experiments. An inducible shRNA system should be established for BYSL loss-of-function experiments in the future.

In summary, our results demonstrate that high levels of BYSL in GBM promote cell migration, invasion, and EMT via the GSK-3 β / β -catenin signaling pathway. These data suggest that BYSL could serve as a biomarker for the invasive subtype of GBM and as a target for the development of anti-GBM drugs.

DATA AVAILABILITY STATEMENT

All datasets generated for this study are included in the article/**Supplementary Material**.

REFERENCES

- Stupp R, Mason WP, Van Den Bent MJ, Weller M, Fisher B, Taphoorn MJ, et al. Radiotherapy plus concomitant and adjuvant temozolomide for glioblastoma. *N Engl J Med.* (2005) 352:987–96. doi: 10.1056/NEJMoa043330
- Wen PY, Kesari S. Malignant gliomas in adults. *N Engl J Med.* (2008) 359:492–507. doi: 10.1056/NEJMra0708126
- Tanaka S, Louis DN, Curry WT, Batchelor TT, Dietrich J. Diagnostic and therapeutic avenues for glioblastoma: no longer a dead end? *Nat Rev Clin Oncol.* (2013) 10:14–26. doi: 10.1038/nrclinonc.2012.204
- Sandberg CJ, Altschuler G, Jeong J, Strømme KK, Stangeland B, Murrell W, et al. Comparison of glioma stem cells to neural stem cells from the adult human brain identifies dysregulated Wnt-signaling and a fingerprint associated with clinical outcome. *Exp Cell Res.* (2013) 319:2230–43. doi: 10.1016/j.yexcr.2013.06.004
- Ishikawa H, Yoshikawa H, Izumikawa K, Miura Y, Taoka M, Nobe Y, et al. Poly (A)-specific ribonuclease regulates the processing of small-subunit rRNAs in human cells. *Nucleic Acids Res.* (2017) 45:3437–47. doi: 10.1093/nar/gkw1047
- Carron C, O'Donohue MF, Choessel V, Faublader M, Gleizes PE. Analysis of two human pre-ribosomal factors, bystin and hTsr1, highlights differences in evolution of ribosome biogenesis between yeast and mammals. *Nucleic Acids Res.* (2011) 39:280–91. doi: 10.1093/nar/gkq734
- Suzuki N, Zara J, Sato T, Ong E, Bakhiet N, Oshima RG, et al. A cytoplasmic protein, bystin, interacts with trophinin, tastin, and cytokeratin and may be involved in trophinin-mediated cell adhesion between trophoblast and endometrial epithelial cells. *Proc Natl Acad Sci USA.* (1998) 95:5027–32. doi: 10.1073/pnas.95.9.5027

ETHICS STATEMENT

The studies involving human participants were reviewed and approved by the Ethics Committee of Xuzhou Medical University. The patients/participants provided their written informed consent to participate in this study.

AUTHOR CONTRIBUTIONS

SG, ZS, and RY conceived the study, participated in its design, and drafted the manuscript. ZS, JZ, and YHW performed the *in vitro* experiments. CL established the GSC cell line. TZ and QM did the experiments related to clinical samples. MP, FY, and YW participated in data analysis. All the authors read and approved the final manuscript.

FUNDING

This work was supported by National Natural Science Foundation of China (Grant Nos. 82072763 and 82002632) and Key Research & Development Plan of Xuzhou City (Grant No. KC20076). SG was supported by the Jiangsu Provincial Six Talents Peak (2019-SWYY-092), Medical Youth Talent (Grant No. QNRC2016787) and Qing Lan projects.

SUPPLEMENTARY MATERIAL

The Supplementary Material for this article can be found online at: <https://www.frontiersin.org/articles/10.3389/fonc.2020.565225/full#supplementary-material>

- Fukuda MN, Miyoshi M, Nadano D. The role of bystin in embryo implantation and in ribosomal biogenesis. *Cell Mol Life Sci.* (2008) 65:92–9. doi: 10.1007/s00018-007-7302-9
- Azzato EM, Driver KE, Lesueur F, Shah M, Greenberg D, Easton DF, et al. Effects of common germline genetic variation in cell cycle control genes on breast cancer survival: results from a population-based cohort. *Breast Cancer Res.* (2008) 10:R47. doi: 10.1186/bcr2100
- Wang H, Xiao W, Zhou Q, Chen Y, Yang S, Sheng J, et al. Bystin-like protein is upregulated in hepatocellular carcinoma and required for nucleogenesis in cancer cell proliferation. *Cell Res.* (2009) 19:1150–64. doi: 10.1038/cr.2009.99
- Godoy H, Mhawech-Fauceglia P, Beck A, Miliotto A, Miller A, Lele S, et al. Developmentally restricted differentiation antigens are targets for immunotherapy in epithelial ovarian carcinoma. *Int J Gynecol Pathol.* (2013) 32:536–40. doi: 10.1097/PGP.0b013e318275a550
- Ayala GE, Dai H, Li R, Ittmann M, Thompson TC, Rowley D, et al. Bystin in perineural invasion of prostate cancer. *Prostate.* (2006) 66:266–72. doi: 10.1002/pros.20323
- Yilmaz M, Christofori G. EMT, the cytoskeleton, and cancer cell invasion. *Cancer Metastasis Rev.* (2009) 28:15–33. doi: 10.1007/s10555-008-9169-0
- Pastushenko I, Blanpain C. EMT transition states during tumor progression and metastasis. *Trends Cell Biol.* (2019) 29:212–26. doi: 10.1016/j.tcb.2018.12.001
- Verhaak RG, Hoadley KA, Purdom E, Wang V, Qi Y, Wilkerson MD, et al. Integrated genomic analysis identifies clinically relevant subtypes of glioblastoma characterized by abnormalities in PDGFRA, IDH1, EGFR, and NF1. *Cancer Cell.* (2010) 17:98–110. doi: 10.1016/j.ccr.2009.12.020

16. Thiery JP. Epithelial-mesenchymal transitions in development and pathologies. *Curr Opin Cell Biol.* (2003) 15:740–6. doi: 10.1016/j.ceb.2003.10.006
17. Jin X, Jeon HY, Joo KM, Kim JK, Jin J, Kim SH, et al. Frizzled 4 regulates stemness and invasiveness of migrating glioma cells established by serial intracranial transplantation. *Cancer Res.* (2011) 71:3066–75. doi: 10.1158/0008-5472.CAN-10-1495
18. Gong A, Huang S. FoxM1 and Wnt/ β -catenin signaling in glioma stem cells. *Cancer Res.* (2012) 72:5658–62. doi: 10.1158/0008-5472.CAN-12-0953
19. Liu Q, Guan Y, Li Z, Wang Y, Liu Y, Cui R, et al. miR-504 suppresses mesenchymal phenotype of glioblastoma by directly targeting the FZD7-mediated Wnt- β -catenin pathway. *Clin Cancer Res.* (2019) 38:358. doi: 10.1186/s13046-019-1370-1
20. Yang W, Wu Pf, Ma Jx, Liao Mj, Wang Xh, Xu Ls, et al. Sortilin promotes glioblastoma invasion and mesenchymal transition through GSK-3 β / β -catenin/twist pathway. *Cell Death Dis.* (2019) 10:208. doi: 10.1038/s41419-019-1449-9
21. Zhang T, Ji D, Wang P, Liang D, Jin L, Shi H, et al. The atypical protein kinase R1OK3 contributes to glioma cell proliferation/survival, migration/invasion and the AKT/mTOR signaling pathway. *Cancer Lett.* (2018) 415:151–63. doi: 10.1016/j.canlet.2017.12.010
22. Li F, Tang C, Jin D, Guan L, Wu Y, Liu X, et al. CUEDC2 suppresses glioma tumorigenicity by inhibiting the activation of STAT3 and NF- κ B signaling pathway. *Int J Oncol.* (2017) 51:115–27. doi: 10.3892/ijo.2017.4009
23. Sun S, Wang Y, Wu Y, Gao Y, Li Q, Abdulrahman AA, et al. Identification of COL1A1 as an invasion-related gene in malignant astrocytoma. *Int J Oncol.* (2018) 53:2542–54. doi: 10.3892/ijo.2018.4568
24. Gao SF, Qi XR, Zhao J, Balesar R, Bao AM, Swaab DF. Decreased NOS1 expression in the anterior cingulate cortex in depression. *Cereb Cortex.* (2013) 23:2956–64. doi: 10.1093/cercor/bhs285
25. Seidel S, Garvalov BK, Acker T. Isolation and culture of primary glioblastoma cells from human tumor specimens. *Methods Mol Biol.* (2015) 1235:263–75. doi: 10.1007/978-1-4939-1785-3_19
26. Du W, Liu Z, Zhu W, Li T, Zhu Z, Wei L, et al. CSN6 promotes tumorigenesis of gastric cancer by ubiquitin-independent proteasomal degradation of p16INK4a. *Cancer Biol Med.* (2019) 16:514–29. doi: 10.20892/j.issn.2095-3941.2018.0410
27. Song Y, Li C, Jin L, Xing J, Sha Z, Zhang T, et al. R1OK2 is negatively regulated by miR-4744 and promotes glioma cell migration/invasion through epithelial-mesenchymal transition. *J Cell Mol Med.* (2020) 24:4494–509. doi: 10.1111/jcmm.15107
28. Willert K, Nusse R. β -catenin: a key mediator of Wnt signaling. *Curr Opin Genet Dev.* (1998) 8:95–102. doi: 10.1016/S0959-437X(98)80068-3
29. Cadigan KM, Nusse R. Wnt signaling: a common theme in animal development. *Genes Dev.* (1997) 11:3286–305. doi: 10.1101/gad.11.24.3286
30. Dorsky RI, Sheldahl LC, Moon RT. A transgenic Lef1/ β -catenin-dependent reporter is expressed in spatially restricted domains throughout zebrafish development. *Dev Biol.* (2002) 241:229–37. doi: 10.1006/dbio.2001.0515
31. Behrens J, Jerchow BA, Würtele M, Grimm J, Asbrand C, Wirtz R, et al. Functional interaction of an axin homolog, conductin, with β -catenin, APC, and GSK3 β . *Science.* (1998) 280:596–99. doi: 10.1126/science.280.5363.596
32. Sheng J, Yang S, Xu L, Wu C, Wu X, Li A, et al. Bystin as a novel marker for reactive astrocytes in the adult rat brain following injury. *Eur J Neurosci.* (2004) 20:873–84. doi: 10.1111/j.1460-9568.2004.03567.x
33. Thiery JP, Acloque H, Huang RY, Nieto MA. Epithelial-mesenchymal transitions in development and disease. *Cell.* (2009) 139:871–90. doi: 10.1016/j.cell.2009.11.007
34. Zeisberg M, Neilson EG. Biomarkers for epithelial-mesenchymal transitions. *J Clin Invest.* (2009) 119:1429–37. doi: 10.1172/JCI36183
35. MacDonald BT, Tamai K, He X. Wnt/ β -catenin signaling: components, mechanisms, and diseases. *Dev Cell.* (2009) 17:9–26. doi: 10.1016/j.devcel.2009.06.016
36. Kunick C, Lauenroth K, Leost M, Meijer L, Lemcke T. 1-Azakenpaulone is a selective inhibitor of glycogen synthase kinase-3 β . *Bioorg Med Chem Lett.* (2004) 14:413–6. doi: 10.1016/j.bmcl.2003.10.062
37. Gonzalez DM, Medici D. Signaling mechanisms of the epithelial-mesenchymal transition. *Sci Signal.* (2014) 7:re8. doi: 10.1126/scisignal.2005189
38. Qin CD, Ma DN, Ren ZG, Zhu XD, Wang CH, Wang YC, et al. Astragaloside IV inhibits metastasis in hepatoma cells through the suppression of epithelial-mesenchymal transition via the Akt/GSK-3 β / β -catenin pathway. *Oncol Rep.* (2017) 37:1725–35. doi: 10.3892/or.2017.5389
39. Sasmita AO, Wong YP, Ling APK. Biomarkers and therapeutic advances in glioblastoma multiforme. *Asia Pac J Clin Oncol.* (2018) 14:40–51. doi: 10.1111/ajco.12756

Conflict of Interest: The authors declare that the research was conducted in the absence of any commercial or financial relationships that could be construed as a potential conflict of interest.

Copyright © 2020 Sha, Zhou, Wu, Zhang, Li, Meng, Musunuru, You, Wu, Yu and Gao. This is an open-access article distributed under the terms of the Creative Commons Attribution License (CC BY). The use, distribution or reproduction in other forums is permitted, provided the original author(s) and the copyright owner(s) are credited and that the original publication in this journal is cited, in accordance with accepted academic practice. No use, distribution or reproduction is permitted which does not comply with these terms.